J Mol Model (2014) 20:2460
DOI 10.1007/s00894-014-2460-9

ORIGINAL PAPER

Theoretical investigations on charge-transfer properties of pentacenequinone derivatives as n-type organic semiconductors

Jun Yin · Yong Hu · Xue-Hai Ju

Received: 26 June 2014 / Accepted: 2 September 2014 / Published online: 16 September 2014

Abstract Electron mobilities of two pentacenquinone derivatives as n-type organic semiconductors, 5,7,12,14-tetraaza-6,13-pentacenquinone (TAPQ5) and 1,4,8,11-tetraaza-6,13-pentacenquinone (TAPQ7), have been investigated at the molecular and crystal levels by means of the density functional theory (DFT) calculations and the incoherent charge-hopping model. It was found that these materials have lower LUMO energy levels, which can easily function as n-type organic semiconductors. The reorganization energy and transfer integral are the two important factors for tuning the electron transfer. The small reorganization energy and the large transfer integral for electron transport suggested that they have relatively high electron mobilities. The transfer integral among the dominant hopping pathways showed that the electron transport processes occur in parallel dimers between two neighboring molecules with π-stacking interactions. On the basis of the angular resolution anisotropic mobility investigation, TAPQ5 and TAPQ7 exhibit remarkable angular dependence of mobilities and anisotropic behaviors. The results are helpful for experimentalists to choose the candidate materials and to design novel organic semiconductors.

Keywords Anisotropic behavior · Density functional theory (DFT) · Electron mobility · n-type organic semiconductors

Introduction

Over the past two decades, organic semiconductors have been the subject of intensive academic and commercial interest due to rapid development of technological applications, such as organic field-effect transistors (OFETs), organic light-emitting diodes (OLEDs), organic photovoltaic cells (OPVs), and various types of sensors [1–3]. Even though charge mobility of organic semiconductors lower than the inorganic semiconductors, they have many desirable properties, such as low cost, light weight, versatility of chemical synthesis, ease of processing, and flexibility [4]. Organic semiconductor materials can be classified as p-type (hole-transporting) or n-type (electron-transporting) according to which type of charge carrier is more efficiently transported through the material [5, 6]. The main parameters to characterize the performance of organic semiconductor are its carrier mobility and on/off current ratio. To be efficient in optoelectronic applications, the carrier mobility (μ) should be at least 0.1 $cm^2 \cdot V^{-1} \cdot s^{-1}$ and the on/off current ratio (I_{on}/I_{off}) should be at least 10^6 [7]. However, the findings of the n-type semiconductors were much less than the p-type ananlogs due to the limited understanding of the fundamental electronic properties of organic semiconductor materials [8]. The n-channel materials are in huge demand, and the comprehensive understanding of the charge transport mechanism in these n-type organic semiconductors is of fundamental interest [9].

To develop high performance n-type organic semiconductors, new designs need to be explored. It is known that quinones act as organic oxidizing reagents in organic synthesis and biological systems due to their lower LUMO energy and the larger electron affinities (EA) [10]. On the basis of this, a large number of novel organic semiconductors have been synthesized, but few studies have explored that the ability to accept electrons links to n-type organic semiconductors [11]. Recently, a few studies have reported that nitrogen-rich heteroquinones incorporated with pyrazine rings are potential n-type organic semiconductors [12–14]. The pentacenequinones with the electron-withdrawing quinone and pyrazine moieties have low-lying and well delocalized

J. Yin · Y. Hu · X.-H. Ju (✉)
Key Laboratory of Soft Chemistry and Functional Materials of MOE, School of Chemical Engineering, Nanjing University of Science and Technology, Nanjing 210094, People's Republic of China
e-mail: xhju@mail.njust.edu.cn

lowest unoccupied molecular orbitals, which are well consistent with n-type organic semiconductors. Mamada and Kumaki et al. [11, 15] have reported that the quinone n-channel organic semiconductors having high electron affinities are very steady in the air atmosphere. In these n-type organic semiconductor materials, there are two special compounds: 5,7,12,14-tetraaza-6,13-pentacenequinone (TAPQ5) and 1,4,8,11-tetraaza-6,13-pentacenequinone (TAPQ7) as shown in Fig. 1. The electron mobilities of TAPQ5 and TAPQ7 were measured from their experiments are in the range of 0.05-0.12 $cm^2 \cdot V^{-1} \cdot s^{-1}$ [16] and $2\text{-}6 \times 10^{-5}$ $cm^2 \cdot V^{-1} \cdot s^{-1}$ [17], respectively.

It is known that the charge transport properties of organic semiconductors are influenced by a series of factors such as mode of crystal packing, film morphology, molecular structure, and material stability, etc. [18, 19]. The crystal packing and molecular structures of TAPQ5 and TAPQ7 are similar. It is believed that the mobility of TAPQ5 should be close to the TAPQ7. However, the electron mobility of TAPQ5 is much larger than that of TAPQ7. In view of this, we perform theoretical calculations to the mobilities of TAPQ5 and TAPQ7 to forecast the possible theoretical values and understand how the interplaying role of various factors affects the charge transport property. Zhang et al. have predicted the electron mobilities of TAPQ5 and TAPQ7 using the four-point method for the mode-specific reorganization energies and the molecular dynamics (MD) simulations for the average electronic couplings [20]. While in this paper, we applied the Marcus-Hush theory to investigate the electron mobilities of TAPQ5 and TAPQ7. In addition, we investigated the electronic properties and charge transport parameters of TAPQ5 and TAPQ7 crystals at the molecular level based on the density functional theory (DFT) calculations coupled with incoherent charge-hopping mechanism model. The results would give insight for the potential n-type semiconductors with high mobility.

Computational details

Although the charge-transfer mechanism in organic crystals is often difficult to determine, the charge-transfer in π-conjugated organic semiconductors with weak intermolecular interactions is generally regarded to occur via the incoherent hopping process [21]. In the incoherent hopping mechanism, the charge carriers are expected to localize and jump between neighboring molecules to migrate across the organic layer. The electron-transfer was represented by the following reactions, respectively:

$$M + M^- \rightarrow M^- + M, \tag{1}$$

where the M and M^- are the neutral molecule and anion, respectively. Besides, as the organic crystals are usually weak polar materials, the charge carrier is fully localized on a single molecule, and the rate of charge transfer between two adjacent molecules, k_i is expressed by Marcus theory [22, 23] as:

$$k_i = \frac{2\pi {t_i}^2}{h}\left(\frac{\pi}{\lambda_- k_B T}\right)^{\frac{1}{2}} \exp\left(-\frac{\lambda_-}{4k_B T}\right), \tag{2}$$

where t_i denotes the transfer integral between neighboring molecules in each individual hopping pathway, and λ_- is the reorganization energy for electron transports, T is the temperature, h and k_B are the Planck and Boltzmann constants, respectively.

According to Eq. 2, we firstly need to compute the λ_- value to calculate the k_i. Generally speaking, the λ_- can be estimated by two methods: (i) the adiabatic potential (AP) energy surface approach [24, 25] and (ii) the normal-mode (NM) analysis method [26, 27], which provides the partition of total relaxation energy into the contribution from each vibration mode. According to the AP scheme, λ_- can be expressed as the following equation [28]:

$$\lambda_- = E_0(Q_-) - E_0(Q_0) + E_-(Q_0) - E_-(Q_-), \tag{3}$$

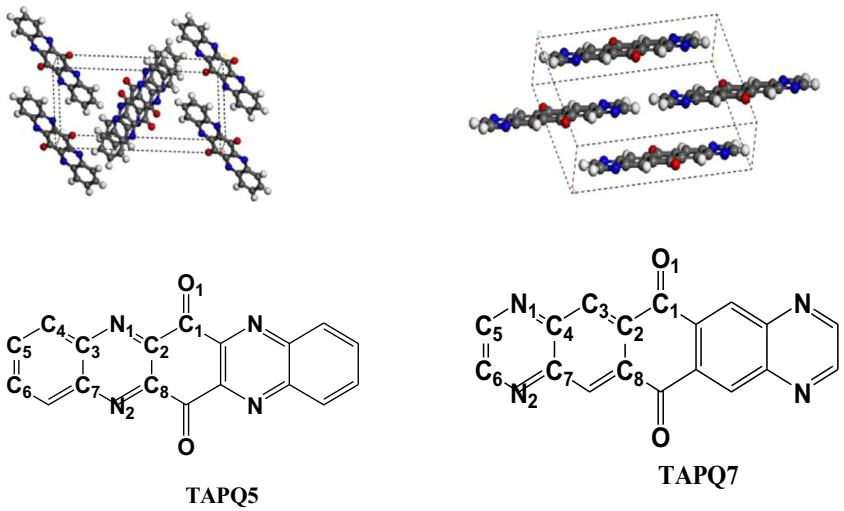

Fig. 1 Crystal (upside) and molecular (below) structures of TAPQ5 and TAPQ7

where E_0 (Q_0) and E_- (Q_-) are the respective energies of optimized neutral and anionic structures, E_0 (Q_-) is the neutral molecular energy with the optimized anionic structure of the molecule, and $E_-(Q_0)$ is the anionic energy with the optimized neutral structure. According to Eq. 2, it can be seen that the electronic coupling t_i is an important parameter determining the rate of charge transfer. In this work, the t_i was calculated on the direct coupling approach, which provides a relatively accurate estimation for the t_i due to considering the spatial overlap between two monomers [29]. In terms of this scheme, the electron coupling is given by:

$$t_i = \frac{h_{12} - \frac{1}{2}(h_{11} + h_{22})S_{12}}{1 - {S_{12}}^2}, \quad (4)$$

where $h_{ij}=\langle\varphi_i|h_{KS}|\varphi_j\rangle$, $S_{ij}=\langle\varphi_i|S|\varphi_j\rangle$, and $|\varphi_i\rangle$ (i=1,2) is the electronic wave function of LUMO for the ith monomer. h_{ij} is the charge transfer integral and S_{ij} is the spatial overlap integral, respectively. h_{KS} is the Kohn–Sham Hamiltonian of the dimer system, which can be calculated by the following equation [30, 31]:

$$h_{KS} = SC\varepsilon C^{-1}, \quad (5)$$

where S is the intermolecular overlap matrix, C is the molecular orbital coefficient matrix from the isolated monomer, and ε is the orbital energy from one-step diagonalization without iteration.

The charge transfer mobility, μ, is then evaluated from the Einstein relation [32]:

$$\mu = \frac{e}{k_B T} D, \quad (6)$$

where e is the elementary charge, k_B is the Boltzmann constant, and D, diffusion coefficient, is a sum of the individual diffusion coefficient along the ith hopping pathway [33]:

$$D = \frac{1}{2n} \sum_i {r_i}^2 k_i P_i, \quad (7)$$

here, n=3 is the space dimensionality, r_i is the centroid distance of the hopping channel i, k_i is the hopping rate of the charge carrier in the ith pathway, and P_i is the relative probability for charge carrier hopping to a particular ith neighbor, which is calculated as by:

$$P_i = \frac{k_i}{\sum_i k_i}. \quad (8)$$

All the quantum chemical calculations were performed with Gaussian 09 package [34].

Results and discussion

Crystal and molecular structures of TAPQ5 and TAPQ7

We optimized the geometries of TAPQ5 and TAPQ7 by the density functional theory with different functionals. The structural parameters of TAPQ5 and TAPQ7 were listed in Tables 1 and 2. It has been demonstrated that the optimized structures are in good agreement with the experimental values at the PBE1PBE/6-31+G(d) level. Therefore, we obtained reorganization energy using this hybrid functional. However, we calculated the electron transfer at the hybrid functional PW91PW91/6-31G(d) level, which has been proved to give good descriptions for electron transfer at the DFT level [35].

As seen in Tables 1 and 2, the optimized bond-lengths and bond-angles for TAPQ5 and TAPQ7 molecules are in good agreement with the experimental values, and the bond-length deviation between them is only about 0.093 Å (the length of C2-N1 for TAPQ5). This result manifests that the PBE1PBE/6-31+G(d) method is quite suitable for elaborating the geometric properties of the investigated materials. The optimized TAPQ5 and TAPQ7 molecules are excellently planar. From the gas phase to the solid phase, bond length and dihedral angle distortions have undergone appropriately. Since the molecular geometry may be somewhat affected by the interaction with surrounding molecules in the solid phase. A further calculation indicates that slight difference in geometry has also little influence on their electronic structures. From

Table 1 Optimized structural parameters and experimental values of TAPQ5 [a]

Parameter	B3PW91	B3LYP	M06-2X	PBE1PBE	Exp [b]
C1-O1	1.21	1.21	1.20	1.21	1.20
C1-C2	1.51	1.51	1.51	1.50	1.50
C3-C4	1.42	1.42	1.42	1.42	1.42
C4-C5	1.37	1.38	1.37	1.37	1.36
C5-C6	1.42	1.42	1.42	1.42	1.41
C3-C7	1.43	1.44	1.43	1.43	1.44
C2-C8	1.43	1.43	1.43	1.43	1.42
C2-N1	1.32	1.32	1.31	1.32	1.32
N1-C3	1.35	1.35	1.35	1.35	1.35
O1-C1-C2	121.65	121.63	121.56	121.63	121.50
C4-C5-C6	120.89	120.89	120.86	120.89	121.00
C1-C2-N1	116.49	116.60	116.47	116.47	116.50
C2-N1-C3	117.24	117.43	117.04	117.16	116.90
N1-C3-C4	119.59	119.69	119.43	119.54	119.70
C3-C4-N5	119.60	119.62	119.56	119.59	119.50

[a] Bond length in Angstrom, bond angle in degree

[b] X-ray in crystal [20]

Table 2 Optimized structural parameters and experimental values of TAPQ7 [a]

Parameter	B3PW91	B3LYP	M06-2X	PBE1PBE	Exp [b]
C1-O1	1.22	1.23	1.22	1.22	1.22
C1-C2	1.49	1.49	1.50	1.49	1.49
C2-C3	1.38	1.38	1.38	1.38	1.37
C3-C4	1.41	1.41	1.41	1.41	1.41
C5-C6	1.42	1.43	1.43	1.42	1.42
C4-C7	1.43	1.43	1.42	1.43	1.42
C2-C8	1.43	1.43	1.43	1.43	1.44
C4-N1	1.36	1.37	1.37	1.36	1.37
N1-C5	1.31	1.31	1.31	1.31	1.31
C1-C2-C3	118.57	118.66	118.47	118.52	119.40
C2-C3-C4	119.40	120.41	120.10	120.30	120.70
C3-C4-N1	119.35	119.44	119.17	119.30	119.40
C4-N1-C5	116.11	116.25	116.10	116.08	115.80
N1-C5-C6	122.68	122.63	122.64	122.69	123.00
O1-C1-C2	121.24	121.18	121.20	121.25	120.80

[a] Bond length in Angstrom, bond angle in degree

[b] X-ray in crystal [20]

Fig. 1, it is straightforward to see that there are two main kinds of packing modes for two adjacent molecules, i.e., face-to-edge and face-to-face packing (π-stacking). Besides, the molecular packings of TAPQ5 and TAPQ7 crystals have a similar π-π stacking and quadruple weak hydrogen bonds [36]. The π-π distances between two neighboring molecules along the pathways (vertical direction) in TAPQ5 (3.89 Å) and TAPQ7 (3.80 Å) are very similar. The large difference of their electron mobilities of TAPQ5 and TAPQ7 has been interpreted by the different morphologies that TAPQ7 has an amorphous film, but TAPQ5 forms a polycrystalline film [17]. In fact, the mobilities strongly depend on the shape and can be covered under different morphologies [37].

Frontier molecular orbitals and electron affinities

The charges were injected from the source electrode to drain electrode into the semiconductor, the current can flow through the transistor channel in OFETs [38]. In order to ensure charge injection from the source electrode effectively, the n-type organic semiconductors should possess low energies of the lowest unoccupied molecular orbital [39]. Based on the optimized structures of the neutral state, the energy levels as well as the electron distribution of the lowest unoccupied molecular orbital (LUMO) and the highest occupied molecular orbital (HOMO) were shown in Fig. 2. As can be seen, the pure PBE1PBE functional combining with the 6-31+G(d) basis set can present confidence in the accuracy of the electronic properties of TAPQ5 and TAPQ7 [20]. The calculated LUMO energies are consistent with the fact that n-type materials

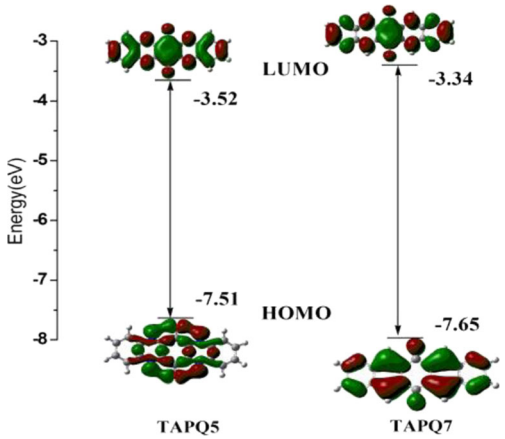

Fig. 2 HOMOs and LUMOs of TAPQ5 and TAPQ7 calculated with PBE1PBE/6-31+G(d) method

typically have LUMO levels between −3 and −4 eV [18]. The calculated LUMO energy, HOMO energy as well as the gap of them for TAPQ5 on this method are −3.52 eV, −7.51 eV, and 3.99 eV, respectively, which are approvingly consistent with the experiment values of −3.78 eV, −6.93 eV, and 3.15 eV [16]. As depicted graphically in Fig. 2, the HOMO and LUMO of TAPQ5 and TAPQ7 distribute to the entire molecule and reveal the typical π-type molecular orbital character, which demonstrates their good carrier transport property. In addition, both TAPQ5 and TAPQ7 with low-lying HOMO and LUMO energies show that they have good carrier injection property. Further investigation exposes the HOMO and LUMO denote a clearly symmetrical distribution in TAPQ5 and TAPQ7. From Tables 1 and 2, we can see that the bond lengths of TAPQ5 are closer to the average bond length than those of TAPQ7. As expected, the electron distribution becomes more delocalized in TAPQ5 than the TAPQ7.

As is known to all, the ionization potential (IP) and the electron affinity (EA) are directly relevant to the air stability. Based on this, the values of EA and IP for TAPQ5 and TAPQ7, both vertical and adiabatic ones were listed in Table 3. According to previous studies, the adiabatic IP of selected air-stable p-type materials ranges from 5.680 eV to 6.786 eV, while the adiabatic EA for n-type ones should be less than 4.0 eV and air-stable n-type ones should be more than 2.80 eV [40, 41]. In light of these viewpoints, TAPQ5 and

Table 3 Calculated ionization potentials (IP) and electron affinities (EA) for TAPQ5 and TAPQ7 (in eV)[a]

Compound	IP(v)	IP(a)	EA(v)	EA(a)
TAPQ5	8.72	8.54	2.19	2.25
TAPQ7	8.95	8.84	2.01	2.08

[a] IP(v)=$E_+(Q_0) - E_0(Q_0)$, IP(a)=$E_+(Q_+) - E_0(Q_0)$, EA(v)=$E_0(Q_0) - E_-(Q_0)$, EA(a)=$E_0(Q_0) - E_-(Q_-)$

TAPQ7 are as n-type materials, but they are unstable as electron transport ones due to the small EA values. Therefore, the suitable operating conditions need to be considered when TAPQ5 and TAPQ7 are applied in practical electron transport OFET devices.

Reorganization energy

According to Eqs. 2, 6 and 7, the reorganization energy λ_ and transfer integral t_i are the two dominant quantities governing the charge mobility. The reorganization energy has both internal and external contributions. The reorganization energy of molecular charge mainly depends on the material differences between neutral and anion state. At this stage, the external part is often neglected, and we only take the internal contribution into account in organic crystals [17, 42–44]. Here we performed the calculation of reorganization energy through the adiabatic potential (AP) energy surface approach. To investigate the performance of different theoretical methods in predicting the reorganization energy for TAPQ5 and TAPQ7, we obtained the reorganization energy using the B3LYP, PBE1PBE, B3PW91, and M06-2X density functionals with 6-31+G(d) basis set. All the reorganization energies of TAPQ5 and TAPQ7 were listed in Table 4. As can be seen in Table 4, the reorganization energies at the PBE1PBE/6-31+G(d) level are 125.4 and 146.6 meV for TAPQ5 and TAPQ7, respectively, which are consistent with the reported values [20], indicating that the PBE1PBE/6-31+G(d) method is valid to describe the reorganization energy. TAPQ5 possesses less reorganization energy than TAPQ7, indicating that the electron delocalization can be promoted by moving the hetero nitrogen atom from the inner ring to the end ring. From the reorganization energy analysis, TAPQ5 is expected to have better charge transport properties than TAPQ7.

Transfer integral

The transfer integral plays an important role in the charge mobility. It is known that transfer integrals are dependent on the molecular arrangement and the overlapping degree of their frontier molecular orbitals [45]. For different crystal structures, the relative positions of the two neighboring molecules involved are entirely different due to different packing structures in crystals. Based on the crystal structures of TAPQ5 and TAPQ7, the electron transfer pathways were illustrated in Figs. 3 and 4. It can be seen that the transport channels of TAPQ5 are featured by the herringbone structure with two directions employing the face-to-edge packing and other directions adopting the face-to-face packing. The overlap for the dimers with the π-π stacking pattern is very large in the short-axis direction, whereas the dimers with face-to-edge stacking are away from each other in the long-axis direction. It is worth noting that TAPQ7 adopts the π-π stacking configurations, but in different transfer pathways, the displacements of the dimers along the long-axis and the short-axis as well as the vertical distances are different. As seen, for TAPQ7, the overlaps of dimers 2 and 5 are less than those of dimers 1, 4 and 3, 6 (see the short axis direction), but the vertical distances of dimers 1, 4 and 3, 6 are much lengthier than the former two dimers. Both the dimers 2 and 5 for TAPQ7 and the dimers in 8 and 12 for TAPQ5 have no overlap though the vertical distances are very small.

We have calculated the electronic couplings for all the dimers and the corresponding values of these electronic couplings were listed in Table 5. As can be seen in Table 5, the electronic couplings along the short-axis (dimers 7 and 11) for TAPQ5 crystal is 63.95 meV, more than five fold of those along other directions, which means that electrons transfer mainly along the one-dimension direction. The same transport properties can also be found in TAPQ7, where electrons transport only along π-

Table 4 Reorganization energy (in meV) for electron transport of TAPQ5 and TAPQ7 using different DFT functionals with the 6-31+G(d) basis set

Compound	B3LYP	PBE1PBE	B3PW91	M06-2X
TAPQ5	122.493	125.381	121.697	152.317
TAPQ7	142.114	146.610	141.372	176.664

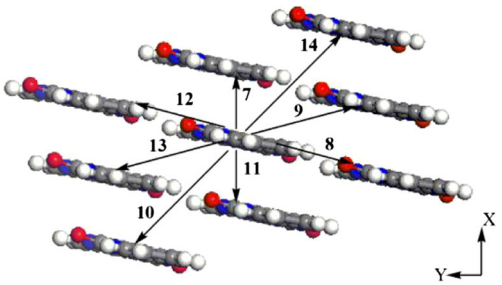

(a)

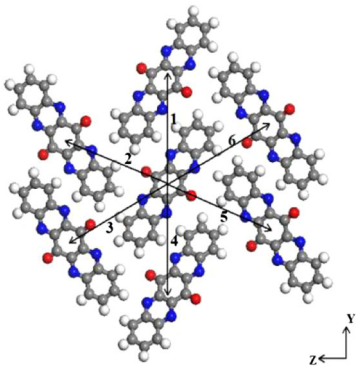

(b)

Fig. 3 Electron transfer pathways for TAPQ5; (**a**) short-axis view and (**b**) long-axis view of TAPQ5

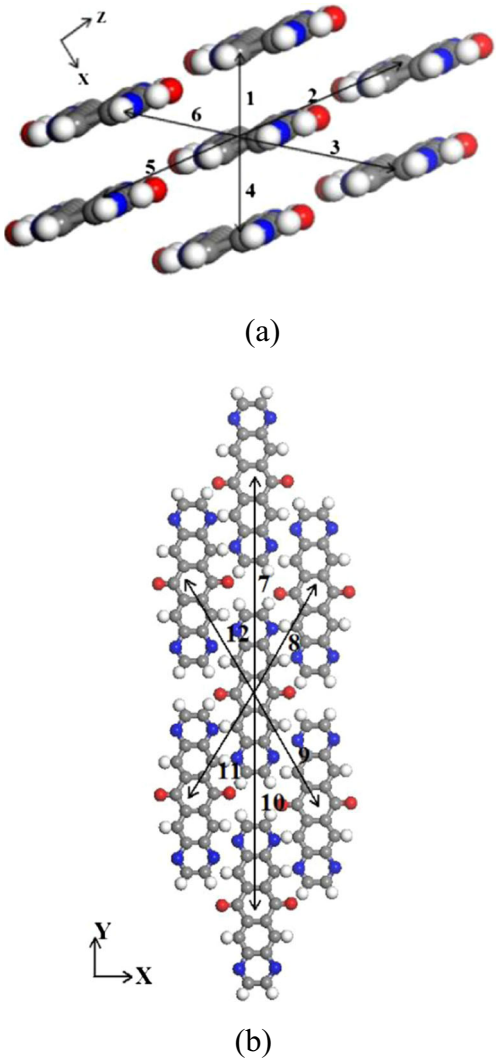

Fig. 4 Electron transfer pathways for TAPQ7; (**a**) short-axis view and (**b**) long-axis view of TAPQ7

stacking dimers 1 and 4. Along the short-axis (dimers 1 and 4) for TAPQ7 crystal is 103.27 meV, which is much larger than those along other directions, demonstrating that the electron mobility of each crystal is mainly determined by one dimensional charge transport. For both TAPQ5 and TAPQ7, the calculated results suggest that the electron transfer along π-stacking is crucial to the charge mobility.

Electron mobility

The electron mobilities of TAPQ5 and TAPQ7 were calculated based on the Einstein equation with values shown in Table 6. It was surprising to find that the calculated mobility of TAPQ7 is much larger than that of TAPQ5. The calculated mobilities of TAPQ5 and TAPQ7 are more than 0.1 $cm^2 \cdot V^{-1} \cdot s^{-1}$, the threshold value fully meets the practical OFET application [5]. Furthermore, the calculated mobility is about ten times larger than experimental values for TAPQ5 [17]. The theoretical

Table 5 Electronic couplings for different molecular pairs in TAPQ5 and TAPQ7 crystals

Pathway	TAPQ5		TAPQ7	
	r [a]	t^{b}_{DA}	r [a]	t^{b}_{DA}
1	9.07	14.01	3.80	103.27
2	10.39	1.63	10.14	2.86
3	10.52	1.77	9.61	8.16
4	9.07	14.01	3.80	103.27
5	10.38	1.63	10.14	2.86
6	10.32	1.77	9.61	8.16
7	3.89	63.95	10.03	3.81
8	9.87	2.99	9.61	8.16
9	9.07	14.01	9.61	8.16
10	9.87	0.01	16.03	3.81
11	3.89	63.95	9.61	8.16
12	9.87	2.99	9.61	8.16
13	9.07	14.01		
14	9.87	0.01		

[a] The distance between two adjacent monomers and the unit is Å

[b] The electronic coupling calculated at PW91PW91/6-31G(d) level and the unit is meV

electron mobility is for the ideal single crystal, while the experimentally measured mobility is for polycrystalline. For TAPQ7, the calculated mobility is also much larger than the experimental value [18]. The small experimental value has been explained by the amorphous film of TAPQ7 with the help of X-ray diffraction patterns [21]. Once the monocrystalline film of TAPQ7 is synthesized, it should have a high mobility. Furthermore, there is a large difference of mobilities between the previous works [20] and our results since the diffusion coefficients were obtained from different methods. Zhang et al. implemented the MD simulation to calculate the diffusion coefficient. Some investigations reported that diffusion coefficient using the MD simulation method is smaller than that by Eq. 7 [46–48]. In addition, the electron mobility in this work refers to room temperature, while Zhang's results were at 400 K [20]. It is noted that our predicted mobilities are closer to the experimental values (Table 6). Besides, the electric field, the charge carrier density and the nuclear tunneling effect also influence the charge transport properties and are quite complicated especially when they are tangled together [49]. As a whole, both TAPQ5 and TAPQ7 crystals

Table 6 Calculated and experimental mobilities of TAPQ5 and TAPQ7 (unit: $cm^2 \cdot V^{-1} \cdot s^{-1}$)

Mobility	TAPQ5	TAPQ7
Calculated	0.52 (1.54)[a]	1.03 (8.75)[a]
Experimental	0.05-0.12	$2\text{-}6\times10^{-5}$

[a] From ref. [20]

have a potential to be further ameliorated to improve the electron mobility.

Anistropic mobility

In the high temperature environment, the strong thermal molecular motions may cause dynamic disorder of molecular disorientation in the crystal structures. This may lead to attenuations, fluctuations, and even enhancements in the intermolecular transfer integrals [43, 49]. As a result, we have investigated the anisotropic effect in TAPQ5 and TAPQ7 to understand how it influences mobility. The angular resolution anisotropic mobility can be calculated by the following equation [48]:

$$\mu_{\Phi} = \frac{e}{2k_BT}\sum_i r_i^2 k_i P_i \cos^2\gamma_i \cos^2(\theta_i - \Phi), \quad (9)$$

where θ_i and γ_i are the hopping angles along the specific transistor channel relative to the reference axis. Φ is the direction of the conducting channel relative to the reference axis (Figs. 5 and 6). We only considered the dimer P in the mobility orientation function on the a–c plane due to the smaller transfer integrals along the dimer T1 and dimer T2 transfer pathways in the TAPQ5 and TAPQ7, that is, the γ_i =0°. As seen from Figs. 5 and 6, the largest electron mobilities are all along or near the 0° and 180° directions relative to the a axis for TAPQ5 and the c axis for TAPQ7, and the directions of their smallest mobilities are perpendicular to the axes mentioned above in the selected planes. The largest mobilities of TAPQ5 and TAPQ7 are 1.68 and 3.13 $cm^2 \cdot V^{-1} \cdot s^{-1}$, respectively, corresponding to the transport pathways with π-π intermolecular interactions. This result suggests that the π-π intermolecular packing is the main driving force to charge transferring.

Conclusions

The geometries, electronic properties, and charge-transport parameters of TAPQ5 and TAPQ7 as organic semiconductors have been theoretically investigated at the molecular and

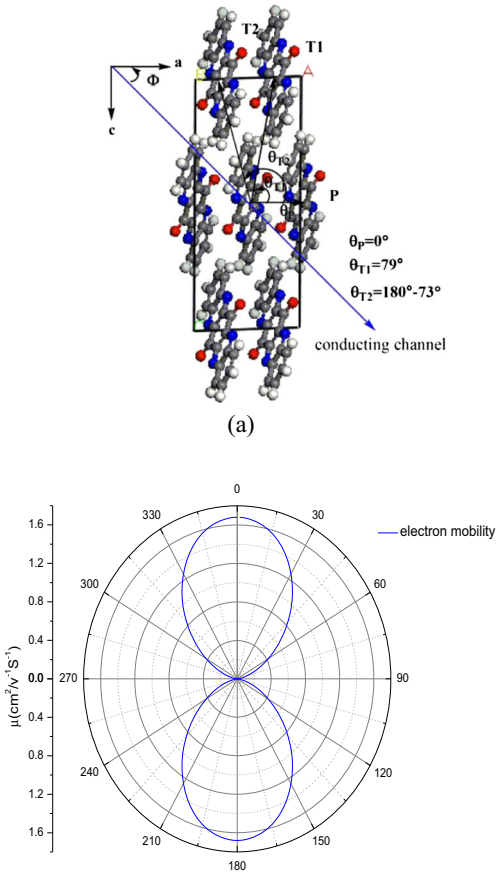

Fig. 5 (**a**) Illustration of projecting different hopping pathways onto a transistor channel in a-c plane of TAPQ5 crystals; θ_P, θ_{T1}, and θ_{T2} are the angles of P, T1, and T2 dimers relative to the reference crystallographic axis a.Φ is the angle along a transistor channel relative to the reference crystallographic axis a. (**b**) The curves of the calculated anisotropic mobilities for TAPQ5

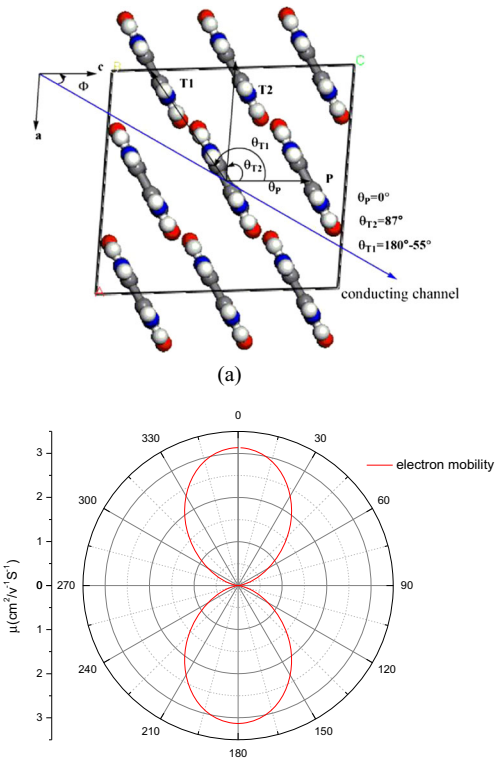

Fig. 6 (**a**) Illustration of projecting different hopping pathways onto a transistor channel in a-c plane of TAPQ7 crystals;, θ_P, θ_{T1}, and θ_{T2} are the angles of P, T1, and T2 dimers relative to the reference crystallographic axis c.Φ is the angle along a transistor channel relative to the reference crystallographic axis c. (**b**) The curves of the calculated anisotropic mobilities for TAPQ7

crystal levels using DFT calculations coupled with the charge-hopping mechanism. The results show that pentacenequinone derivatives, which have low-lying and delocalized LUMOs, can easily function as n-type organic semiconductors. Besides, the reorganization energy and the transfer integral significantly contribute to the dramatic change of the electron mobility. The transfer integral calculations among the dominant hopping pathways show that the electron transport processes occur in parallel dimers between two neighboring molecules with π-stacking interactions for TAPQ5 and TAPQ7. Furthermore, compared to the measured values, the theoretical values of mobilities are much larger, indicating that the experimental mobilities could be further increased by crystallizing the OSC molecules into an ordered lattice, reducing the contact resistance and/or using an alternative method of sample preparation.

Acknowledgments The authors thank the National Science Foundation of China (No. 21372116) for supporting this work.

References

1. Friend RH, Gymer RW, Holmes AB, Burroughes JH, Marks RN, Taliani C, Bradley DDC, Dos Santos DA, Brédas JL, Lögdlund M, Salaneck WR (1999) Nature 397:121
2. Nagamatsu S, Kaneto K, Azumi R, Matsumoto M, Yoshida Y, Yase K (2005) J Phys Chem B 109:9374
3. Someya T, Katz HE, Gelperin A, Lovinger AJ, Dodabalapur A (2002) Appl Phys Lett 81:3079
4. Drury CJ, Mutsaers CMJ, Hart CM, Matters M, de Leeuw DM (1998) Appl Phys Lett 73:108
5. Usta H, Facchtti A, Marks TJ (2011) Acc Chem Res 44:501
6. Wen Y, Liu Y (2010) Adv Mater 22:1331
7. Katz H, Bao Z (2000) J Phys Chem B 104:671
8. Meng H, Bao Z, Wang BC, Mujsce AM (2001) J Am Chem Soc 123: 9214
9. Gershenson ME, Podzorov V, Morpurgo AF (2006) Rev Mod Phys 78:973
10. Facchetti A, Yoon MH, Stern CL, Katz HE, Marks TJ (2003) Angew Chem Int Ed 42:3900
11. Mamada M, Kumaki D, Nishida J, Tokito S, Yamashita Y (2010) ACS Appl Mater Interfaces 2:1303
12. Winkler M, Houk KN (2007) J Am Chem Soc 129:1805
13. Miao S, Appleton AL, Berger N, Barlow S, Marder SR, Hardcastle KI (2009) J Chem Eur 15:4990
14. Wang H, Wen Y, Yang X, Wang Y, Zhou W, Zhang S, Zhan X, Liu Y, Shuai ZG, Zhu DB (2009) ACS Appl Mater Interfaces 1:1122
15. Mamada M, Nishida J, Tokito S, Yamashita Y (2009) Chem Commun 15:2177
16. Tang Q, Liang Z, Liu J, Xu J, Miao Q (2010) Chem Commun 46: 2977
17. Liang Z, Tang Q, Liu J, Li J, Yan F, Miao Q (2010) Chem Mater 22: 6438
18. Murphy AR, Fréchet JM (2007) Chem Rev 107:1066
19. Coropceanu V, Cornil J, Filho DA, Olivier Y, Brédas JL (2007) Chem Rev 107:926
20. Zhang WW, Zhong XX, Zhao Y (2012) J Phys Chem A 116:11075
21. Hanwell MD, Madison TA, Hutchison GR (2010) J Phys Chem A 114:20413
22. Marcus RA (1993) Rev Mod Phys 65:599
23. Barbara PF, Meyer TJ, Ratner MA (1996) J Phys Chem 100:13148
24. Malagoli M, Brédas JL (2000) Chem Phys Lett 327:13
25. Liu T, Troisi A (2011) J Phys Chem C 115:2406
26. Brédas JL, Beljonne D, Coropceanu V, Cornil J (2004) Chem Rev 104:4971
27. Zhang MX, Chai S, Zhao GJ (2012) Org Electron 13:215
28. Kapturkiewicz A, Herbich J, Karpiuk J, Nowacki J (1997) J Phys Chem A 101:2332
29. Mohakud S, Alex AP, Pati SK (2010) J Phys Chem C 114: 20436
30. Gao HZ, Qin CS, Su ZM, Wang Y (2008) J Phys Chem A 112:9097
31. Yin SW, Yi YP, Li QX, Shuai ZG (2006) J Phys Chem A 110:7138
32. Cornil J, Lemaur V, Calbert JP, Brédas JL (2002) Adv Mater 14:726
33. Deng WQ (2004) W A Goddard 108:8614
34. Frisch MJ, Trucks GW, Schlegel HB, Scuseria GE, Robb MA, Cheeseman JR, Scalmani G, Barone V, Mennucci B, Petersson GA et al (2009) Gaussian 09, Revision A.1. Gaussian Inc, Wallingford
35. Huang J, Kertesz M (2004) Chem Phys Lett 390:110
36. Yang GC, Si YL, Wu QX, Su ZM (2011) Theor Chem Acc 128:257
37. Brédas JL, Norton JE, Cornil J, Coropceanu V (2009) Acc Chem Res 42:1691
38. Reimers JR (2001) J Chem Phys 115:9103
39. Li HX, Shi Q (2012) J Phys Chem A 116:11886
40. Liu CC, Mao SW, Kuo MY (2010) J Phys Chem C 114:22316
41. Chang YC, Kuo MY, Lu HF, Chao I (2010) J Phys Chem C 114: 11595
42. Wang LJ, Li QK, Shuai ZG, Chen LP, Shi Q (2011) Adv Mater 23: 1145
43. Jones BA, Facchetti A, Marks TJ, Wasielewski MR (2007) Chem Mater 19:2703
44. Wang X, Lau KC (2012) J Phys Chem C 116:22749
45. Chen XK, Guo JF, Zou LY, Ren AM, Fan JX (2011) J Phys Chem C 115:21416
46. Zhao CB, Wang WL, Yin SW, Ma Y (2013) New J Chem 37:2925
47. Yang XD, Wang LJ, Wang CL, Long W, Shuai ZG (2008) Chem Mater 20:3205
48. Di Motta S, Di Donato E, Negri F, Orlandi G, Fazzi D, Castiglioni C (2009) J Am Chem Soc 131:6591
49. Yin S, Lv Y (2010) Adv Mater 160:1241